Werk

Übergeordnetes Werk

Terms and Conditions

Contact

Niedersächsische Staats- und Universitätsbibliothek Göttingen
Georg-August-Universität Göttingen
Platz der Göttinger Sieben 1
37073 Göttingen
Germany
Email: gdz@sub.uni-goettingen.de

Zeitschrift für Geophysik, 1970, Band 36, Seite 399—420. Physica-Verlag, Würzburg

Investigation of the Auroral Electrojet

By H. HEINRICH, D. REIMER and H. SIEMANN, Braunschweig[1])

Eingegangen am 25. März 1970

Summary: The program PEJ 1, supported by the German Government, was planned in 1967 to investigate the Auroral Electrojet (AEJ). Three rockets of the Black Brant III-type with magnetometers for measuring the field components, an impedance-probe and a retarded-potential analyzer on board were launched in late 1968 from ESRANGE in Kiruna, Sweden.

A position-finding system, based on magnetometer measurements was used to calculate the position of the ionospheric current-system and to control the count-down.

The gross structure of the AEJ was resolved by comparing the available data from ground-based magnetometers with the height-profiles of the total intensity.

Above an altitude of 130 km a sudden change in the phase shift of the transverse magnetic field has been measured. This can be interpreted as being due to a magnetospheric current system that is closed in the ionosphere. From the height profiles of the electron density the conductivities were computed. The electric fields as derived from the combined results of these data and from the magnetometer measurements are comparable to results obtained by barium-cloud experiments.

Zusammenfassung: Im November und Dezember 1968 wurden auf dem Gelände der ESRO (European Space Research Organisation) in Kiruna, Schweden, drei Raketen vom Typ Black Brant III (Programm PEJ 1) gestarted mit dem Ziel, den mit magnetischen Baystörungen am Erdboden verbundenen stark gebündelten Teil (Polarer Elektrojet) des ionosphärischen Strom-Systems zu erforschen.

Die Raketen waren mit Magnetometern zur Messung der Komponenten des Erdfeldes, mit einer Impedanzsonde zur Erfassung der lokalen Elektronendichte und einem Bremsfeld-analysator zur Ermittlung der Elektronentemperatur und der Geschwindigkeiten geladener Teilchen ausgerüstet worden.

Zur Bestimmung der Position des Strom-Systems ist ein auf Magnetometerregistrierungen basierendes automatisches Ortungssystem benutzt und zur Kontrolle des count-down eingesetzt worden.

Die großräumige Struktur des Polaren Elektrojet (PEJ) konnte durch Vergleiche von Magnetometerregistrierungen am Boden mit den Höhenprofilen der Total-Intensität abgeleitet werden.

Oberhalb 130 km wurde eine starke Änderung der Phasenverschiebung des transversalen Magnetfeldes beobachtet. Diese Änderung kann als Effekt eines magnetosphärischen Stromsystems, welches durch die Pedersen-Ströme in der Ionosphäre geschlossen wird, gedeutet werden. Aus den Elektronendichte-Profilen sind die Leitfähigkeiten berechnet worden. Die kombinierten Ergebnisse von Magnetometern und Impedanzsonde liefern für die elektrischen Felder Werte, die mit den Ergebnissen von Barium-Wolken-Experimenten vergleichbar sind.

[1]) Dr. H. HEINRICH: Institut für Geophysik und Meteorologie Techn. Universität Braunschweig. — Dr. D. REIMER and Dr. H. SIEMANN: Institut für Geophysik und Meteorologie Techn. Universität Braunschweig; Present address: Dornier System, Friedrichshafen.

1. General Introduction

Geomagnetic bay disturbances seem to be closely correlated with auroral displays [AKASOFU 1968], the most exciting physical phenomena in the auroral zone, although magnetic bays have been observed with no visible auroras occuring. This means that the ionospheric currents which are responsible for the observed magnetic disturbances need not be confined to auroral displays, and there is some evidence for the north-south extension of these ionospheric currents to be several 100 km.

Until now only a few direct measurements habe been performed to study such current-systems while most of the investigations concerning ionospheric current-systems are based on ground-based magnetometer data [AKASOFU et al. 1969].

Our aim was to investigate the most intense part of the current-system near local midnight which we call Auroral Electrojet (AEJ), to find out its structure and to get an idea of what may be the driving force of that current-system.

Ionospheric electric fields appear to be the dominant driving forces, so a good deal of rocket experiments have been performed to measure the ionospheric electric fields in the polar region [HAERENDEL and LÜST 1968; POTTER and CAHILL 1969; WESCOTT, STOLARIK and HEPPNER 1969].

In addition, there exist a few model-calculations of the AEJ [BOSTRÖM 1964; BONNEVIER, BOSTRÖM and ROSTOKER 1969] in which ionospheri electric fields are employed. These calculations are the theoretical background of our work, therefore a short review is being given here.

1.1 *The models of the AEJ*

Let us assume the driving force of the AEJ to be an electric field which originates in the magnetosphere.

Due to the high parallel conductivity in the magnetosphere the magnetic field lines are equipotentials. Thus, any magnetospheric electric field will be mapped down into the ionosphere along the field lines if we disregard effects possibly caused by an ionospheric dynamo. We shall discuss two configurations and ask for important differences which may be detected by the instruments on board of a rocket.

To compute the height profiles of the Hall- and Pedersen-conductivities [FEJER 1965] one has to know the height variations of the electron density and collision frequencies of the particles involved in this process [DALGARNO 1961, NICOLET 1953].

Although the measured profiles of the electron density [KIST and SPENNER 1970] may considerably differ from this function it does not affect appreciably the shape of the height profiles of the conductivities under consideration.

In our considerations we shall employ height-integrated terms on account of the fact that the electric field is nearly height-independent [see BOSTRÖM 1964].

Configuration I

Figure 1 shows a schematic representation of this model. We introduce a coordinate-system x, y, z (x-axis pointing north, y-axis east, and z-axis positive towards the earth's centre) in which the current flows from east to west over a length of several hundred km, at least. Its north-south extension is taken to be 10 km, its vertical extension depends on the conductivities. The primary electric field E is homogeneous in the region of the AEJ and no currents will flow to and from the magnetosphere.

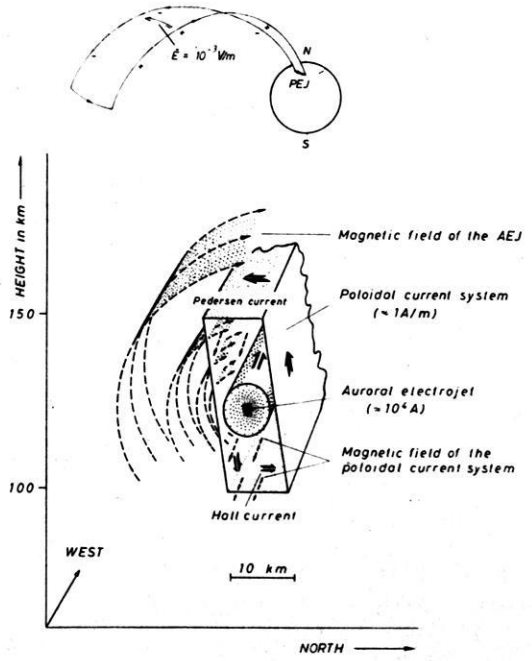

Fig. 1: Schematic representation of currents and magnetic fields for configuration I [SEILER und KERTZ 1967].

The Hall current of the field E will charge the boundaries of the current layer, and give rise to a polarization-field E_p, the Hall current of which is responsible for the large enhancement of I_y, thus producing an electrojet (I_y is the y-component of the height-integrated current density).

The most interesting aspect of this configuration is the generation of an ionospheric poloidal current-system surrounding the electrojet. This poloidal system is the source of a horizontal magnetic field which is directed to the East and confined to an altitude-range between about 100 km and 160 km.

Configuration II

The primary electric field E is now directed north-south and confined to the current-layer while currents may flow to and from the magnetosphere.

In this model the electrojet is simply the Hall current of the field E. On the other hand the Pedersen-current of this electric field is part of a magnetospheric poloidal current system that produces a horizontal magnetic field which is directed to the west and might be detectable up to great heights. Figure 2 shows a schematic representation for the second configuration.

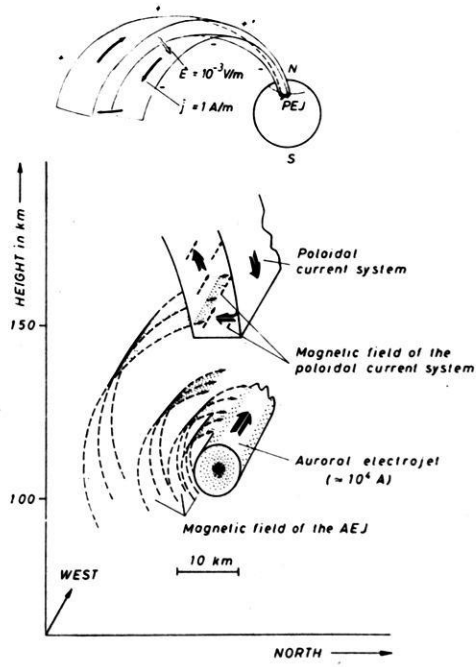

Fig. 2: Schematic representation of currents and magnetic fields for configuration II [SEILER und KERTZ 1967].

The remarkable difference between the two configurations concerning the horizontal fields produced by the poloidal current systems establishes an effective means to distinguish between the two models on the base of rocket magnetometer measurements. We therefore decided to launch three rockets (the description of the experiments are given in sections 3 and 4, see also [KIST and SPENNER 1970] to yield some information about the gross structure of the jet, the driving forces, and, with a few reasonable assumptions, the magnitude of the ionospheric electric fields.

The results of ground based measurements are presented in section 2. The results from the rocket magnetometers are given in section 3 and 4, and the close connection of the results in section 2 and 3 should be mentioned. The flight performance of the rockets and magnetograms are given in the appendix.

2. The Position-Finding System for the AEJ

2.1 *Introduction*

The magnetic fields of the poloidal current systems of configurations I and II were to be measured to get the desired informations about the driving mechanism of the AEJ. Thus the AEJ itself,—for the moment we consider the AEJ to be a line current—, must be located within the rocket trajectory. This requires an accurate position-finding system (PFS) for the AEJ.

The main features of our system (PFS), which is based on magnetometer measurements, will be briefly discussed in this section.

2.1.1 Model current systems

For simplicity we assume that the measured magnetic disturbances at the earth's surface represent the field of a single line current in the ionosphere.

Then we find

$$Z/H = -d/h \tag{2-1}$$

Z = vertical component of the earth's field
H = horizontal component of the earth's field
X = north component of the earth's field
Y = east component of the earth's field
d = distance between observation point and the current
h = height of the current

The cartesian coordinate system we use throughout this paper gives heights above ground level as negative values. The direction $\alpha + 90°$ of the auroral electrojet will be calculated from

$$\operatorname{tg}\alpha = Y/X \tag{2-2}$$

(α being rotated in a clockwise sense).

On account of the fixed trajectory for a given type of rockets at ESRANGE, Kiruna, the rocket reaches the altitude of 100 km a well known time after take off. Thus if we know the position and velocity of the AEJ at any time, we are able to determine the exact launch time to meet the conditions mentioned in chapter 2.1.

Provided the AEJ is a single line current in the *E*-region, we only need one magnetometer station to yield the required information about d, $\varkappa$, and the current strength I of the system.

In reality there are several complicating factors:

a) The AEJ is not a line current. Ground-based magnetometers on a north-south-profile often measure almost identical horizontal disturbances over several degrees of latitude.

b) One has to account for the induction effect of the well-conducting earth.

c) Pulsations and effects with time scales of e.g. one day are unwanted pertubations.

To take these pertubations into consideration the PFS should consist of more than one station, because more than three parameters may be determined to calculate d, α and I.

We decided to use two stations. Thus a model of the AEJ may contain six parameters for a unique solution.

2.1.2 The model for the AEJ

KERTZ [1954] has shown that the field of a line current I_L at height h_L equals the field of a plane current at height h exactly if the current distribution is

$$i_h(x)=\frac{I_L}{\pi}\cdot\frac{h-h_L}{(x-x_0)^2+(h-h_L)^2}\,. \tag{2-3}$$

The half-width of this distribution is $2\,b = 2\,(h - h_L)$ and the total current is

$$\int_{-\infty}^{+\infty} i_h(x)\,dx = I_L\,.$$

To account for point a) in chapter 2.1.1 we assume that the AEJ has the distribution given in (2—3), and we may use the equivalent line current I_L for the calculation of d, α and I.

To account for points b) and c) we use the differences of corresponding components of two stations and allow for a homogeneous field (H_0, Y_0, Z_0 are the field-components) in all components. The advantage of this method is that the homogeneous field contains all the fields the sources of which are at great distances as compared to the distance of the ground stations. Daily variations and ring current effects are eliminated as well as the influence of deep-seated induced currents. For detailed information see REIMER [1969].

2.2 *The position-finding system*

For fast accurate calculations a small computer was used. The setup of the whole system is specified in the block-diagram of figure 3.

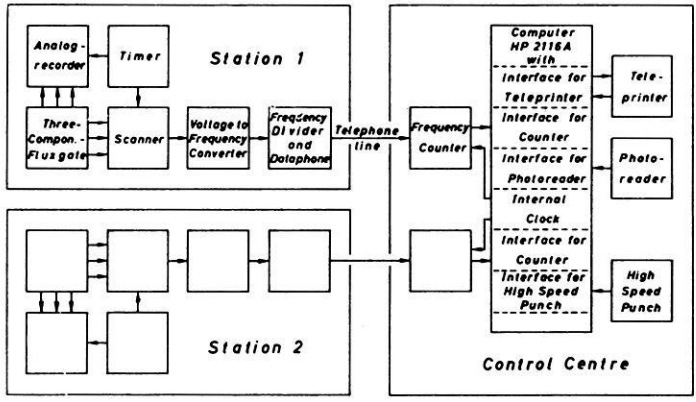

Fig. 3: Block diagram for the position-finding system with two identical magnetometer stations.

As magnetometers we used two sets of three-component fluxgates with a range of $\pm 2000\,\gamma$ and an electrical suppression of the normal fields. The block containing the three sensors was oriented such that one component was perpendicular to the horizontal magnetic field during quiet periods. The sensors and the boxes containing the electronics were buried about 50 cm below the earth's surface to eliminate drifts possibly caused by variations of temperature. A calibration could be done in situ by applying a dc-current to the feed-back coil of the magnetometers. For more information see MÜLLER [1970].

2.3 *Results from ground-based measurements*

2.3.1 Height integrated current densities

During the campaign recordings of the magnetic field have been taken at the five stations Kiruna, Abisko, Tromsö, Esrange and Kilpisjärvi (120 km north of ESRANGE), the last two being used in the position-finding system. The recordings of the last two stations are shown in the appendix for the times of the three rocket flights. These magnetograms were employed in a detailed study in which the height-integrated current densities were determined on the basis of more sophisticated models for the AEJ. The most complex model allowed for two independent equivalent line currents and their induced currents. Thus up to nine parameters had to be evaluated. This was done using a least-squares-fit and an iterative method. The results for rockets 1 and 2 are shown in figures 4 and 5 for the launchings on Nov. 19., 2h 38m 30s, and on Dec. 4., 23h 26m 30s. It must be pointed out again that the current density functions shown are derived solely from ground-based measurements. This means that variations on scales less than about 100 km could not be detected. Significant features are the great half-width of the current-distributions of the order of 500 km and perhaps the asymmetry

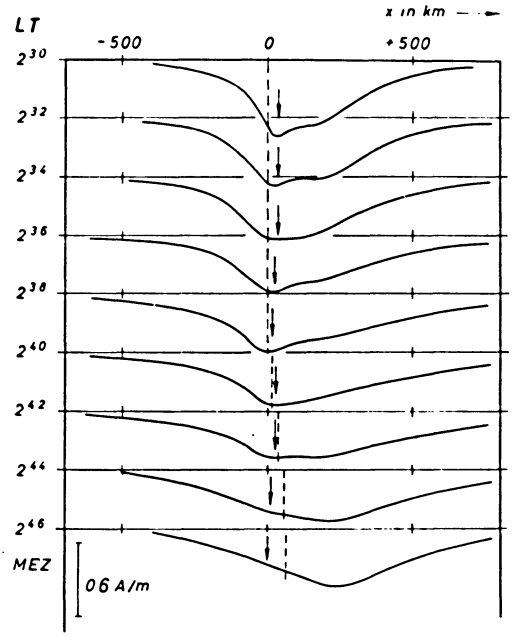

Fig. 4: Height-integrated current densities for flight of rocket 1 (19. 11. 1968).
The dashed lines illustrate the horizontal distance of the rocket from the launch-site.
The arrows show the results of the position-finding of the AEJ.

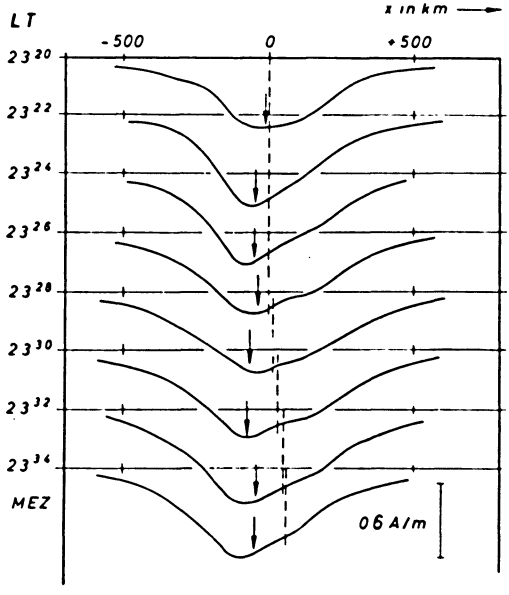

Fig. 5: Height-integrated current densities for flight of rocket 2 (4. 12. 1968).
The dashed lines illustrate the horizontal distance of the rocket from the launch-site.
The arrows show the results of the position-finding of the AEJ.

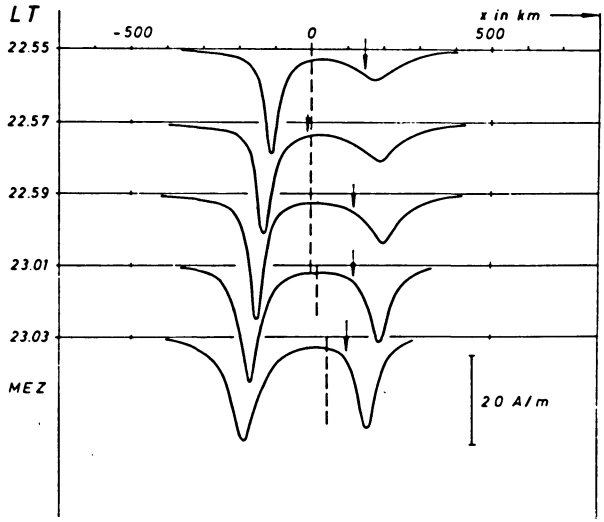

Fig. 6: Height-integrated current densities for flight of rocket 3 (3. 12. 1968). The dashed lines illustrate the horizontal distance of the rocket from the launch-site. The arrows show the results of the position-finding of the AEJ.

To check the validity of the deduced current distributions, more calculations have been done. Good agreement with the rocket measurements of the total intensity of the magnetic field was found.

2.3.2 Result from the PFS

Small arrows in figures 4 and 5 indicate the position of the equivalent line current as determined from the records of only two stations. The arrows point to small maxima of the current distribution which are superimposed on the very wide general distribution. This performance was expected as the model allowed for a single equivalent line current and a homogeneous field.

The limits of the model are shown during the flight of rocket 3 launched on Dec. 3., 22h 59m 00s. The investigations based on all the accessible ground-level measurements yield a current distribution with two strong and narrow peaks (figure 6). The rocket passed through the current-carrying layers halfway between the two maxima. The position-finding system—forced to interpret the measurements as belonging to one equivalent line current—sometimes pointed to one maximum, and sometimes to the other one.

So we may conclude that the system actually used, and the model with a homogeneous field and one equivalent line current did work and did give reliable results as long as the overall distribution of height-integrated current density could be approximated by the function given in (2-3).

To allow for more complicated structures a model containing two equivalent line currents and perhaps their induced currents should be used. This model requires ground-based measurements from at least three stations.

3. The Results of the Proton-Magnetometer Measurements

3.1 *Introduction*

3.1.1 The rocket-instrument

In the proton-magnetometer the well known effect of nuclear energy-level splitting by a magnetic field is used to derive the total strength of the earth's magnetic field by simply measuring the Larmor frequency.

It was calculated that for the maximum weight and resistance allowed a magnetometer probe of width 5 cm and length 10 cm yields optimum signal strength of the voltage induced in the receiver coil. A sensor of these dimensions, filled with butylalcohole which has a relaxation-time of 0.9s, and a coil with 2300 windings were used. This combination yielded an ac-signal of $10\,\mu V_{pp}$ across the matched input of the amplifier.

The amplifier was composed of high-reliability operational elements and a relais-switching circuit with electronic control during the various switching steps. The amplified signal was fed into the IRIG-Standard telemetry and recorded at the surface together with a 200 kHz-reference ground station signal.

3.1.2 Data processing

To obtain the total intensity of the earth's field the frequency of a decaying sine wave has to be measured with a high degree of accuracy.

To eliminate the noise from the record the data had to be digitized first and then subjected to a (digital) high-pass filter, because no appropriate analog device was available.

Subsequently, the "hyper-rapid Fourier transform" was used to compute the spectrum of each signal. The frequency at the spectral peak—which is the relevant information—was found by applying some interpolation formula.

Careful tests with exactly known sets of simulated data were performed to check the whole procedure. It turned out to be accurate within $\pm 10\,\gamma$. On account of the perturbation fields of the payload and the rocket itself several reductions were made. Thus, the absolute accuracy of the measured data depends solely on the accuracy to which the perturbation fields are known—which is $\pm 50\,\gamma$—whereas the relative accuracy equals that of the data-processing procedure.

The effect of the rocket spin on the Larmor-frequency was eliminated. For further information see HEINRICH [1969].

3.2 *Measurements and Interpretation*

3.2.1 Height-Profiles of ΔF

ΔF is the difference between the measured total intensity and the corresponding value calculated from a spherical harmonics expansion (Program FIELD and set 12/66 of coefficients) of the earth's magnetic fields.

The next three figures, 7, 8 and 9 show plots of ΔF versus altitude for the three rocket flights.

To interpret these results we shall first look at the possible current-distribution as given in section 2 and derive a three-dimensional current-distribution on the base of these data which is in agreement with the electron-density results [KIST et al., 1970]. Finally we shall compute the magnetic field of this current-system, and, by selecting the component in the direction of the earth's field, we will try to fit the measurements.

3.2.2 The magnetic field of a three dimensional current-system

As pointed out in section 2, we can easily calculate the field-components of a line current. This magnetic field may be produced as well by some equivalent current-distribution at a certain height.

For further calculations we assume the maximum current-density (concerning the height variations) to be at the 110 km level, where the maximum electron-density was measured.

The height variation of the current density corresponds to that of the conductivities. We therefore introduce a Chapman-function, $CF(h)$, to describe the height variations of the current-density.

Using the notation of section 2 we may write

$$j(h,x)=\frac{I_L}{\pi}\frac{b}{(x-x_0)^2+b^2}\cdot CF(h) \tag{3-2}$$

(with j being the current-density within the electrojet system). After an integration we obtain I_L, the strength of the equivalent line current.

The magnetic field of this model electrojet had to be computed numerically.

3.2.3 Interpretation of the results

Rocket 1

From the appropriate height-integrated current densities that were given in section 2 (cf. fig. 4) we calculated the magnetic field along the rocket trajectory, and compared the result with the proton-magnetometer data. A better agreement was achieved after the original distribution had been modified slightly. These changes (of amplitude, position and half-widths of the peaks) were well within the limits of resolution given

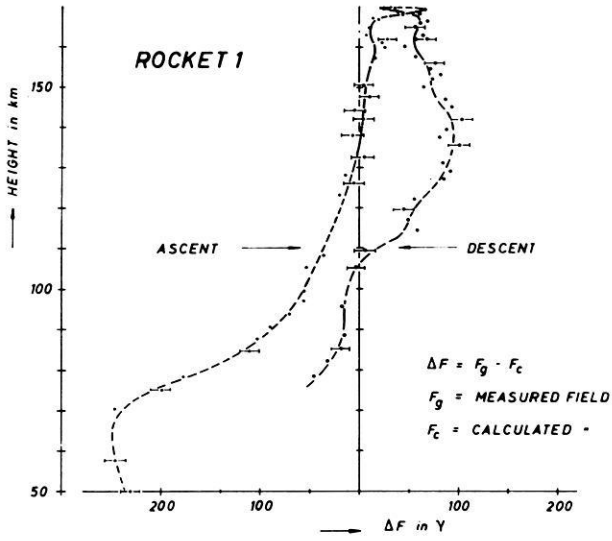

Fig. 7: Results from the proton-magnetometer measurements for rocket 1.

in section 2. The time variation of the modified distribution is shown on the right-hand side of fig. 10. The other graph shows the computed magnetic field $\tilde{F}$ of this current distribution along the rocket trajectory.

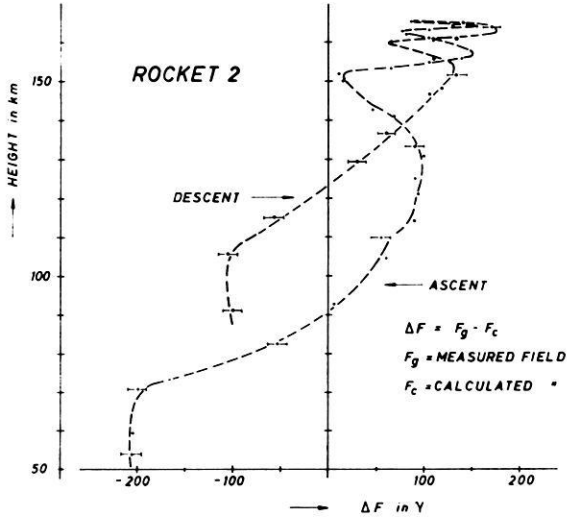

Fig. 8: Results from the proton-magnetometer measurements for rocket 2.

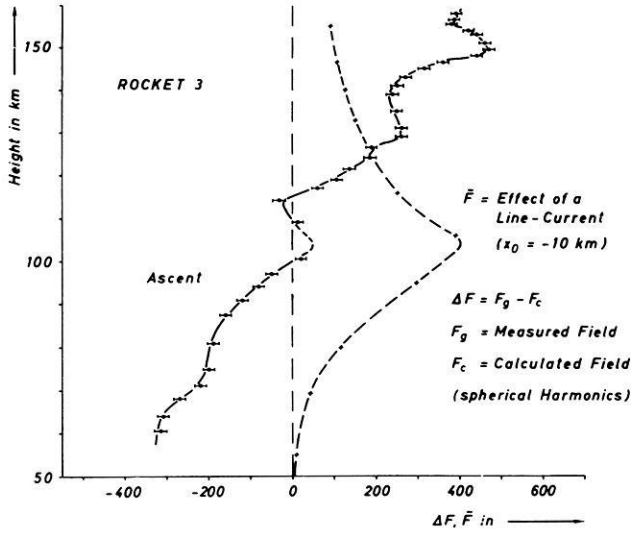

Fig. 9: Results from the proton-magnetometer measurements for rocket 3.

A comparison of this result with the ΔF-curve in figure 7 clearly demonstrates the really good agreement of the measurements and the calculations.

Among the variety of distributions that can be derived from ground-based data, the distribution we chose for figure 10 describes very well the distribution at those times. Yet, we de not claim to have given the exact values of amplitude, position and half-width, since some other combination of two—ore even more—current-systems might yield similar results. However, the shape of the combined system may not be altered much from that given in fig. 10 in order to fit the ΔF curve as good as in this case.

Rocket 2

When we applied the trial-and-error method described above to the data for rocket 2 we found that the current distribution as given in fig. 5 had to be altered more distinctly than in the first case:

The half-width of the northern current band had to be reduced to about one half of the value deduced from ground-based measurements (see also KIST and SPENNER [1970]).

Figure 11 shows the result. Apart from the rapid changes in the measured curve above 130 km—which we believe are due to rapid motions of the southern current-system on a small scale—the calculated curve again shows the same features as the measured curve in figure 8, so the same conclusion as for rocket 1 holds.

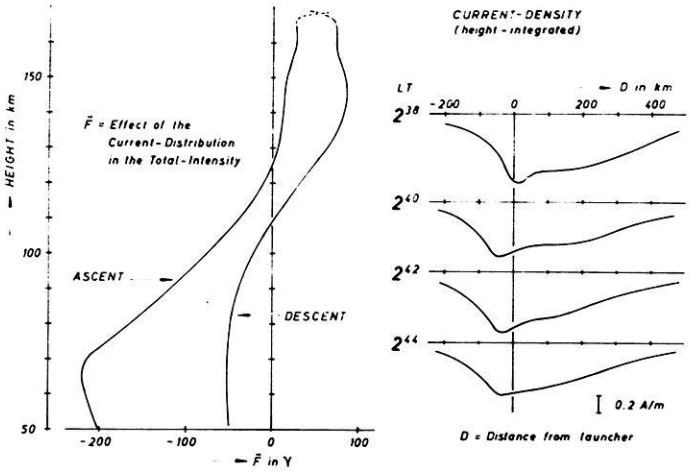

Fig. 10: The magnetic field of the current distribution on the right side (rf. fig. 4) yields a component $\tilde{F}$ in the direction of the earth's magnetic field. $\tilde{F}$ is shown on the left side and should be compared with fig. 7.

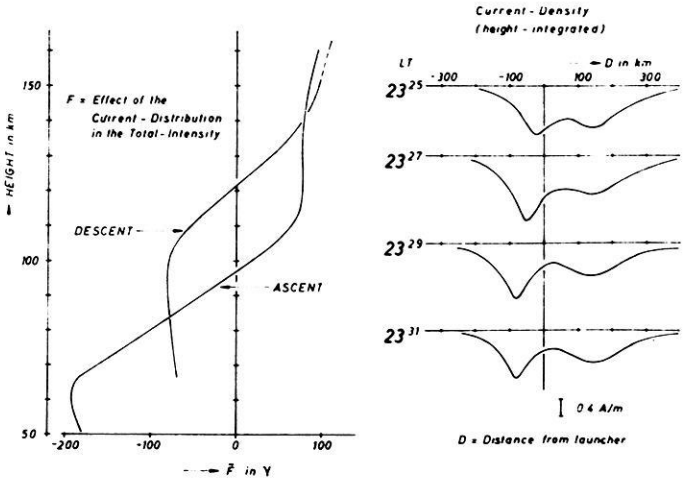

Fig. 11: The magnetic field of the current distribution on the right side (rf. fig. 5) yields a component $\tilde{F}$ in the direction of the earth's magnetic field. $\tilde{F}$ is shown on the left side and should be compared with fig. 8.

Rocket 3

Because of the telemetry breakdown no data were available for the descent part of the trajectory. On account of the various possibilities to fit the ΔF curve given in fig. 9 no model calculations have been performed in this case.

According to the ground-based results, the rocket passed the current-system in between two strong bands (cf. fig. 6). The position and amplitudes of the peaks are somewhat uncertain, because the small values recorded on the ground had to be interpreted as being differences of large contributions of either current band. No wonder then, that the ground-based data do not show all details that can be deduced from the rocket magnetometer data. For instance, an analysis of fig. 9 displays an asymmetry of the current concentration that is not shown in fig. 6. It is easily visualized that the field produced by a current-distribution, which is centered approximately 40 km south of the launch-site and which looks like a line current (10 km south of launch-site), nicely fits the data. The southern current appears to have been stronger as well as lying closer to the rocket trajectory than the northern current band.

4. The Results of the Search-Coil Magnetometer Measurements

4.1 *Introduction*

4.1.1 Description of the Instrument

The sensor of the search-coil magnetometer was a flat coil with a diameter of 12 cm which had 13000 windings and was mounted in such a way that its axis was perpendicular to the spin axis of the rocket. Because of the rocket's rotation in the geomagnetic field an alternating voltage was induced in the coil. Its amplitude and phase yielded the projection of the magnetic field vector into a plane normal to the spin axis. The signal was amplified and fed to an analog-to-digital converter.

4.1.2 Calibration of the Magnetometer

Although metal parts were avoided in the vicinity of the search-coil a distortion of the measurements (especially concerning the phase) by eddy currents had to be expected. Therefore the magnetic frequency response of the magnetometer was determined with the instrument mounted in the payload. Braunbek-Coils were used to generate homogeneous alternating fields, and digital data processing techniques were employed [SCHNEBEL 1970].

4.1.3 Data Processing

First the PCM-signal delivered by the analog-to-digital converter had to be decoded. Then with the aid of a digital computer, the amplitude and phase of the quasi-

sinusoidal signal were determined as functions of time. These time functions were corrected by taking into account frequency response obtained during the dynamic calibration of the built-in magnetometer.

4.1.4 Separation of the disturbance caused by the AEJ from the undisturbed field

Unfortunately, at the time the payload had been constructed there was no device available which allowed the rocket's attitude to be determined with respect to some coordinate systems fixed to the earth. Thus the permanent part of the geomagnetic field could be eliminated only by assuming that neither the attitude nor the spin rate changed during flight. Because of the aerodynamics of the rocket this is probably only true for altitudes higher than 100 km. Therefore only data from measurements taken above this level have been processed.

Due to the nearly vertical attitude of the rocket axis the amplitude of the signal is about the absolute value of the horizontal field component. The undisturbed horizontal field component measured along the rocket trajectory as a function of time

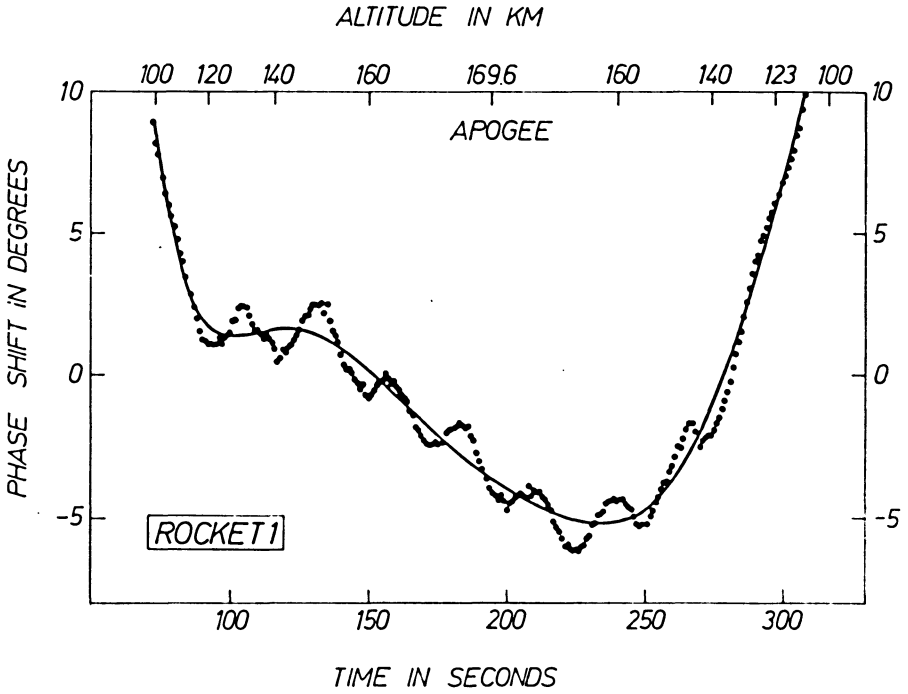

Fig. 12: The dotted curve represents the measured phase shift of the transverse magnetic field versus flight time, the solid line is obtained after correction for nutation effects.

would be a parabola because the altitude of the rocket as a function of time has this shape and the apogee is very small compared to the earth's radius. Therefore the permanent part of the measured field component is assumed to be a parabola found by a least-squares polynomial approximation, and the effect of the AEJ is given by the deviation from this curve.

By analogy the effect of the AEJ on the signal's phase is the deviation from a straight line, also obtained from a least-squares approximation.

Now the amplitude deviation as well as the deviation in phase still contain an approximately sinusoidal part which is caused by the coning motion of the rocket. This distortion was removed by approximating the time function by a polynomial of the 10th degree. The effect of this procedure on the phase shift is shown in fig. 12.

4.2 *Measurement and Interpretation*

4.2.1 Horizontal Intensity

The pertubation of the horizontal intensity, caused by the AEJ, as measured with the search-coil magnetometer agrees with the results from the measurements of the total field intensity. As these measurements have been discussed in detail in chapter 3.2, a discussion of the measured horizontal intensity is being omitted here.

4.2.2 Direction of the Horizontal Component

As outlined in section 1, BOSTRÖM [1964] developed several models to explain the phenomenon of the AEJ, the two most important of which were shown in fig. 1 and 2. Both models include a poloidal current system, which generates a horizontal magnetic field that cannot be detected on ground but can be measured with rocket magnetometers.

Configuration I

Contains a poloidal current system which causes a horizontal magnetic field of some 1000 γ pointing east between 100 km and 160 km altitude.

Configuration II

Contains a poloidal current system which causes a horizontal magnetic field of some 1000 γ pointing west above 130 km altitude.

When the horizontal intensity of the undisturbed field (pointing to the north) is 10000 γ, an additional field of 1000 γ shifts the field direction about ± 5 degrees.

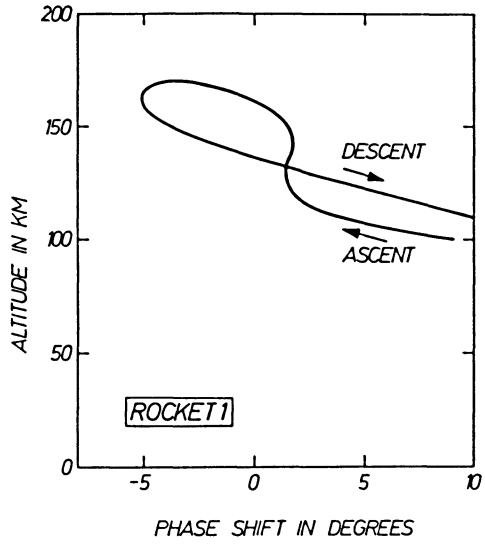

Fig. 13: Phase shift as a function of altitude for rocket 1.

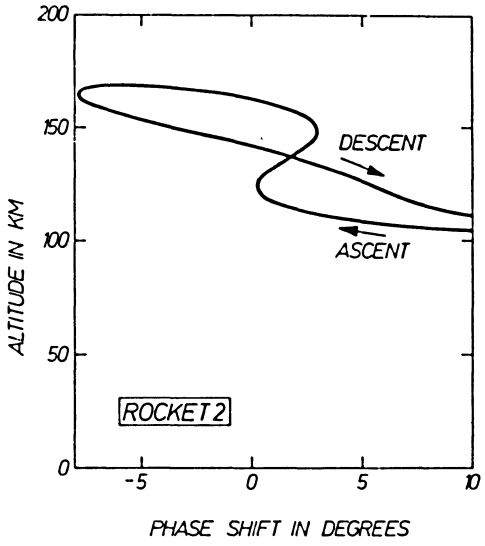

Fig. 14: Phase shift as a function of altitude for rocket 2.

This means:

If the measurements of the search-coil magnetometer show a phase shift of some 5 degrees in the range between 100 km and 160 km one should accept configuration I. If the measurements of the search-coil magnetometer show above about 130 km a phase shift of some 5 degrees one should accept configuration II.

Figure 13 and figure 14 show the phase shifts observed during flight 1 and flight 2, respectively, as a function of altitude.

Unfortunately ascent und descent do not show nearly the same values as one would expect. This means that the spin rate of the rocket was not sufficiently constant as had been presumed for the method of data processing described above.

But when we look at the ascents, in which one can trust more than in the descents because of the aerodynamics of the rockets, we observe a sudden change in the phase shift above 130 km.

5. Conclusions

As had been expected it was possible to determine the center of the horizontal distribution of a current system with the position-finding system.

In connection with data from several observatories the measurements yielded a broad horizontal distribution in all three cases. For flights 1 and 2 an asymmetric distribution was found. For flight 3 the shape of the distribution was determined by two large maxima separated by at least 200 km.

The structure of the AEJ was determined by the proton-magnetometer data with a resolution much higher than any one that could have been obtained from the ground-based measurements.

In addition, the altitude of the AEJ could be determined by the proton-magnetometer data. The measurements supported the assumption of the position-finding procedure that the altitude of the AEJ ranges between 100 and 120 km.

The results of the search-coil suggest that Boström's configuration II (cf. sect. 1) might describe the AEJ mechanism quite well on account of the measured sudden change in the phase shift above an altitude of 130 km.

The combined results from magnetometer and electron-density measurements yielded electric fields in the ionosphere comparable to those obtained from ion-cloud experiments.

The spin frequency and the attitude of the rockets were not sufficiently constant between 80 km and 130 km (due to unknown effects, perhaps aerodynamics) as had been presumed for the method of data processing described in sec. 4. Thus a very precise attitude measurement system and an accurate determination of the spin frequency together with the component-magnetometers are necessary equipment for further investigations of the AEJ. In addition, the apogee of the rocket should be above a height of 250 km.

To get a precise picture of the ionospheric conditions during a magnetic bay-disturbance one must include simultaneous measurements of the ionospheric electric fields. The results of these combined measurements would yield the desired information about the unknown source mechanisms involved.

Although one might be afraid of the technical complexity of a project like this, we suppose that further investigations of the AEJ are urgent and we hope that our results will have a stimulating effect.

Acknowledgements

We are indebted to the German Bundesministerium für Bildung und Wissenschaft for financial support, and to a team of the Deutsche Forschungs- und Versuchsanstalt für Luft- und Raumfahrt, who have launched the rockets, for technical assistance. We wish to thank Prof. Dr. RAWER and Messrs. R. KIST and K. SPENNER for their excellent cooperation, and Prof. Dr. W. KERTZ for his helpful advice and comments during the course of this program.

The success of this project is due to the outstanding efforts of our co-workers Messrs. D. SCHNEBEL, B. KRÜGER, B. THEILE and S. MÜLLER in our team.

Appendix

A. Flight performance of the rockets.

	Day	launch-time	apogee	remarks
Rocket 1	19. 11. 68	02h 38m 30s LT	169 km	
Rocket 2	4. 12. 68	23h 26m 30s LT	167 km	
Rocket 3	3. 12. 68	22h 59m 00s LT	168 km	telemetry breakdown near apogee

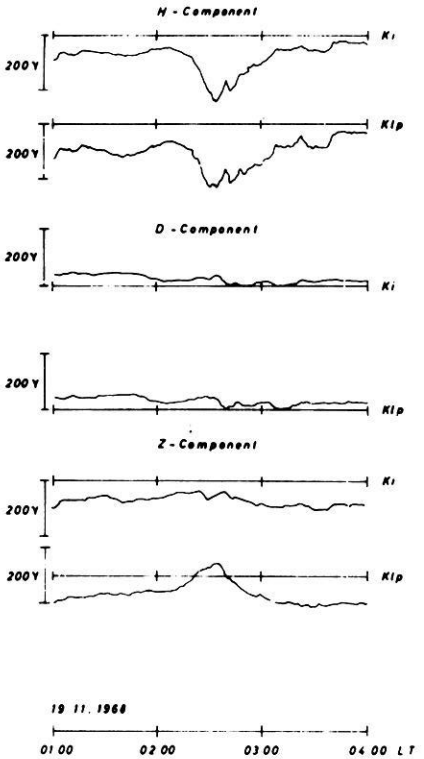

Fig. 15: Magnetograms from Kiruna (Ki) and Kilpisjärvi (Klp) for november 19., 1968 (rocket 1).

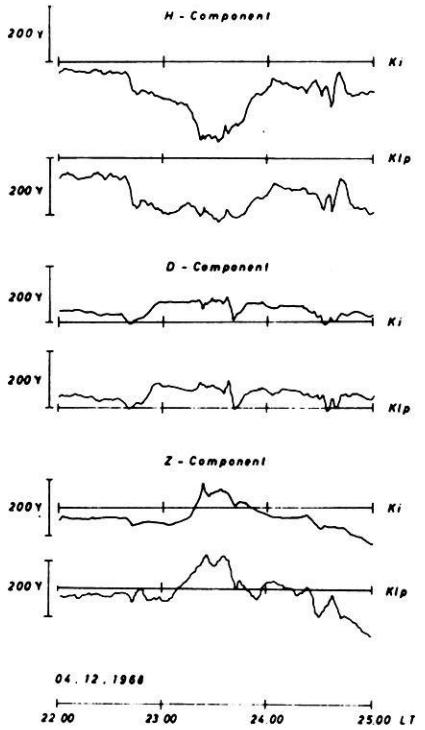

Fig. 16: Magnetograms from Kiruna (Ki) and Kilpisjärvi (Klp) for december 4., 1968 (rocket 2).

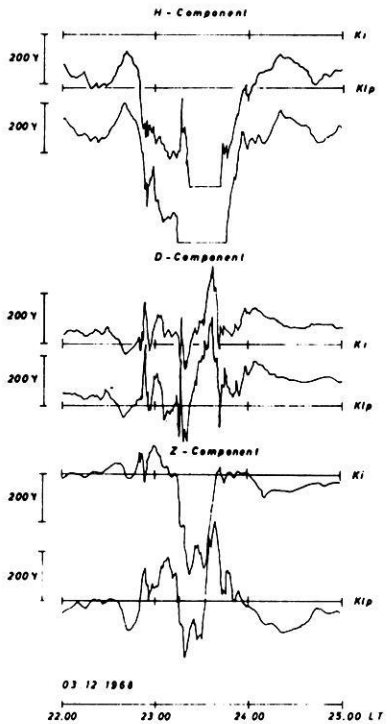

Fig. 17: Magnetograms from Kiruna (Ki) and Kilpisjärvi (Klp) for december 3., 1963 (rocket 3).

References

AKASOFU, S.-I.: Polar and Magnetospheric Substorms. D. Reidel Publishing Comp., Dordrecht, 1968

AKASOFU, S.-I., and C.-I. MENG: A study of polar magnetic substorms 2. Three-dimensional current system. J. Geophys. Res. 74, 4035–4053, 1969

BONNEVIER, B., G. ROSTOKER, and R. BOSTRÖM: A Three-dimensional model current system for polar magnetic substorms. Publication of the Royal Institute of Techn., Stockholm. Dept. of Plasma Physics, May 1969

BOSTRÖM, R.: A model of the auroral electrojet. J. Geophys. Res. 69, 4983–4999, 1964

DALGARNO, A.: Charged particles in the upper atmosphere. Ann. Géophys. 17, 16–49, 1961

FEJER, J. A.: Motions of Ionisation. In Physics of the Earth's Upper Atmosphere (ed. Hines, Phagis, Hartz, Fejer), 157–175, Prentice-Hall, Inc., Englewood Cliffs, N. Y., 1965

HAERENDEL, G., and R. LÜST: Electric fields in the upper atmosphere. In Earth's Particles and Fields (ed. B. M. McCormac), 271–285, Reinhold Book Corp., New York, 1968

HEINRICH, H.: Raketenmessung in der Polarlichtzone mit einem Protonen-Magnetometer. GAMMA 6, Techn. Universität Braunschweig, 84 S., 1969

KERTZ, W.: Modelle für erdmagnetisch induzierte elektrische Ströme im Untergrund. Nachr. Akad. Wiss. Göttingen IIa, 101–110, 1954

KIST, R., und K. SPENNER: Plasmamessungen im Polarlicht-Elektrojet und daraus erschlossene elektrische Felder. Z. Geophys., this issue, 1970

MÜLLER, S.: 3-Komponenten-Magnetometer zur Peilung des polaren Elektrojet. GAMMA 11, Techn. Universität Braunschweig, 1970

NICOLET, M.: The collision frequency of electrons in the ionosphere. J. Atm. Terr. Phys. 3, 200–211, 1953

POTTER, W. E., and L. J. CAHILL: Electric and magnetic field measurements near an auroral electrojet. J. Geophys. Res. 74, 5159–5160, 1969

REIMER, D.: Bestimmung der momentanen Lage des polaren Elektrojets. GAMMA 9, Techn. Universität Braunschweig, 151 S., 1969

SCHNEBEL, D.: Verfahren zur Kalibrierung von Raketen-Magnetometern. GAMMA 10, Techn. Universität Braunschweig, 1970

SEILER, E., und W. KERTZ: Der polare Elektrojet. Z. Geophys. 33, 371–402, 1967

WESCOTT, E. M., J. D. STOLARIK, and J. P. HEPPNER: Electric fields in the vicinity of auroral forms from motions of barium vapor releases. J. Geophys. Res. 74, 3469–3487, 1969